

Sampling and Reconstruction of Sparse Signals in Shift-Invariant Spaces: Generalized Shannon's Theorem Meets Compressive Sensing

Tin Vlašić and Damir Seršić

Abstract

This paper introduces a novel framework and corresponding methods for sampling and reconstruction of sparse signals in shift-invariant (SI) spaces. We reinterpret the random demodulator, a system that acquires sparse bandlimited signals, as a system for acquisition of linear combinations of the samples in the SI setting with the box function as the sampling kernel. The sparsity assumption is exploited by compressive sensing (CS) framework for recovery of the SI samples from a reduced set of measurements. The samples are subsequently filtered by a discrete-time correction filter in order to reconstruct expansion coefficients of an observed signal. Furthermore, we offer a generalization of the proposed framework to other sampling kernels that lie in arbitrary SI spaces. The generalized method embeds the correction filter in a CS optimization problem which directly reconstructs expansion coefficients of the signal. Both approaches recast an inherently infinite-dimensional inverse problem as a finite-dimensional CS problem in an exact way. Finally, we conduct numerical experiments on signals in B-spline spaces whose expansion coefficients are assumed to be sparse in a certain transform domain. The coefficients can be regarded as parametric models of an underlying continuous signal, obtained from a reduced set of measurements. Such continuous signal representations are particularly suitable for signal processing without converting them into samples.

This research was supported in part by the European Regional Development Fund under the grant KK.01.1.1.01.0009 (DATACROSS) and in part by the Croatian Science Foundation under the project IP-2019-04-6703.

T. Vlašić and D. Seršić are with the Department of Electronic Systems and Information Processing, University of Zagreb Faculty of Electrical Engineering and Computing, Unska 3, HR-10000 Zagreb, Croatia (e-mail: tin.vlasic@fer.hr; damir.sersic@fer.hr).

This work has been submitted to the IEEE for possible publication. Copyright may be transferred without notice, after which this version may no longer be accessible.

Index Terms

B-spline, compressive sensing, inverse problem, sampling theory, shift-invariant spaces, sparse signal recovery

I. INTRODUCTION

Sampling theorems are an essential tool that allows for processing of real-world signals on a digital processor. Due to its elegance and practicality, the Nyquist-Shannon theorem [1], [2] is the most prevalent sampling theorem. It states that a signal must be sampled at the rate that is at least twice the highest frequency contained in the signal. However, real-world signals are rarely exactly bandlimited and can often be much better represented in alternative bases [3], [4] other than Fourier. This led to a generalization of Shannon’s sampling theorem to other classes of functions. In particular, the concept extends nicely to the spline and wavelet spaces in which signals are expressed as a linear combination of the integer shifts of a generator [5]–[7]. Sampling of signals in shift-invariant (SI) spaces resembles Shannon’s sampling theorem with additional discrete-time correction filtering of samples which are not necessarily pointwise values of the signals. Unlike the *sinc* function, spline and wavelet generators have finite support, which makes the reconstruction formula in the SI sampling theorem feasible. In an SI sampling setting, a signal is sampled at least at the signal’s rate of innovation, and similarly to the conventional sampling theorem, it is challenging to build sampling hardware that operates at a sufficient rate when the rate of innovation is high.

Recently, sparsity has received growing attention in the field of signal processing. It lies at the heart of compressive sensing (CS) [8]–[12], a sampling and reconstruction paradigm that has been extensively researched over the past decade. The goal of discrete CS is to recover a signal $\mathbf{x} \in \mathbb{R}^N$ from linear measurements $\mathbf{y} \in \mathbb{R}^M$ given by $\mathbf{y} = \Theta \mathbf{x}$, where $\Theta \in \mathbb{R}^{M \times N}$ is a sensing matrix and $M < N$. The exact recovery from such an underdetermined inverse problem is possible if the signal is Q -sparse, i.e. it has at most $Q \ll N$ nonzero entries, and under certain conditions [13], [14] on the sensing matrix Θ . The problem can efficiently be solved by a number of greedy or convex optimization algorithms [15]. While CS reduces the number of measurements sufficient for perfect recovery of the signal, and consequently the sampling rate, it increases the computational complexity of the reconstruction.

The vast majority of papers concerning CS focus on discrete inverse problems. Since the most of real-world signals are continuous, there are many works that extend discrete CS to the analog domain. These works mostly rely on a discretization or heuristics in order to adopt an infinite-dimensional inverse problem to a finite CS setting. The discrete model Θ of a continuous measurement process is often an approximation, which introduces errors in the system. However, some papers are focused on solving

infinite-dimensional CS problems [16]–[20]. Furthermore, hardware realizations for CS of analog signals were proposed in [21]–[25]. Alternative approaches that aim to solve continuous inverse problems are in fields of super-resolution [26]–[28] and finite rate of innovation [29]–[31]. These approaches are typically based on the assumption that a signal or its certain order of derivative consists of finite number of Dirac delta functions per unit of time and the goal is to recover exact location of the jumps at super-resolution.

We propose a framework for CS of analog signals that lie in an arbitrary shift-invariant space. The model we treat is infinite-dimensional, as the unknown signal is a function $f : \mathbb{R} \rightarrow \mathbb{R}$. Although the signal in an SI space is continuous, it is uniquely characterized by a sequence of coefficients, which makes a discretization method elegant. We show that the continuous-domain inverse problem can exactly be recast as a finite-dimensional CS problem. Initially, we develop a CS system based on the front-end configured as a parallel version of the random demodulator (RD) [32]. The RD’s high-rate pseudo-random sequence can be reinterpreted as a combination of the box sampling functions in the conventional SI setting. Integration and sub-Nyquist sampling that follow demodulation produce samples that are linear combinations of several samples in the standard SI setting. The SI samples are recovered by solving a finite-dimensional CS problem prior to filtering by a discrete-time correction filter in order to reconstruct the signal. Furthermore, we extend the measurement process of the proposed framework to arbitrary sampling functions with a finite support. The front-end configuration remains the same with an only difference in the sampling kernel. For this type of a continuous inverse problem, we propose a reconstruction procedure in which the discrete-time correction filter is embedded in a finite-dimensional CS problem. Solving the proposed CS problem directly recovers expansion coefficients that characterize the signal. In numerical experiments, we demonstrate the effectiveness of the proposed framework by using the B-splines, but the method is not solely limited to the spline spaces. This manuscript is a more fully developed publication based on a conference paper [33].

The main contributions of the paper are:

- We reinterpret the random demodulator, a system that acquires sparse bandlimited signals, as a system for sampling and reconstruction of signals that lie in an arbitrary shift-invariant subspace;
- We show that the inherently continuous inverse problem can be discretized into a finite-dimensional problem of compressive sensing type in an exact way;
- We introduce a novel framework for reconstruction of signals in shift-invariant spaces acquired by a parallel version of the random demodulator. The signal is reconstructed by combining compressive sensing and the shift-invariant reconstruction procedure. The proposed framework significantly reduces the sampling rate for sparse signals in shift-invariant spaces;
- We offer a generalization of the proposed sampling and reconstruction method to other sampling

kernels that lie in arbitrary shift-invariant spaces. In order to reconstruct acquired signals, we propose a method that embeds correction filtering in a CS problem;

- We conduct the proposed framework on signals that are synthetically made Q -sparse and real-world signals. We provide the experimental results of our methods in which signal models lie in B-spline spaces.

The remainder of the paper is organized as follows. In Section II, we relate our work to the findings of other studies. We provide a short review on sampling in SI spaces and an infinite-dimensional formulation of a CS problem in Section III. In Section IV, we reinterpret the random demodulator as a system that allows for CS of a wide class of signals in an SI subspace. We propose a measurement model that discretizes the continuous-domain measurements of the RD in an exact way. In Section V, a framework for reconstruction of signals in shift-invariant spaces acquired by a parallel version of the random demodulator is proposed. In Section VI, we offer a generalization of the proposed method to other sampling kernels. Numerical experiments are provided in Section VII and we conclude the paper in Section VIII.

II. RELATED WORK

The random demodulator [32], [34] is a sampling system that is used to acquire sparse bandlimited signals. The RD demodulates a signal by multiplying it with a high-rate pseudo-random sequence of ± 1 s, referred to as the chipping sequence. The chipping sequence switches between the levels ± 1 at the Nyquist rate. The demodulated signal is lowpass filtered prior to being sampled at a low rate. The lowpass filter is an integrator that integrates the demodulated signal between taking two successive samples. After each sample is taken, the integrator is being reset. The mixer that runs at the Nyquist rate can be easily designed using inverters and multiplexers. The most critical part for the speed of the mixer and the bottleneck of the system is the settling times of inverters and multiplexers to reach steady state [32]. The modulated wideband converter (MWC) [35], [36] is a CS type front-end for acquiring of multiband signals with unknown band locations. Basically, the MWC is a parallel version of the RD with lowpass filters instead of integrators that follow demodulation. The authors consider the MWC for sampling of a sparse multiband signal supported on N frequency bands, with at most $Q \ll N$ bands active. To be able to successfully reconstruct the signal, the MWC should consist of at least M parallel channels, where $2Q \leq M < N$ [35]. The main idea behind the RD and the MWC is aliasing of the spectrum, in such a way that each spectrum band appears in the baseband, before sampling at a low rate. The reconstruction is possible due to the sparse harmonic or band support.

In [37], Eldar introduces a method for CS of analog signals in a union of shift-invariant subspaces. Sparsity is modeled by assuming that only Q out of N generating functions are active. Conventionally,

such signals are acquired using N parallel sampling filters prior to sampling at a rate $1/T$, leading to a system with sampling rate N/T . Eldar shows how to sample such signals at a rate much lower than N/T by using M sampling filters, where $2Q \leq M < N$. Expansion coefficients of SI subspace bases share a joint sparsity pattern and are recovered using the infinite measurement vector model [38]. The method can be extended to a special case of sampling of signals that lie in an SI space spanned by a single generator with a periodic sparsity pattern, i.e. out of consecutive group of N coefficients, there are at most Q nonzero expansion coefficients, in a given pattern. Each integer shift of the generator in a period NT is modeled as a single subspace. The unknown signal is prefiltered by a set of M sampling functions that are weighted linear combinations of the shifts of a function biorthogonal to the generator [37], leading to a system with sampling rate $M/(NT)$, where $2Q \leq M < N$. Sampling filters that are linear combinations of biorthogonal functions may be quite difficult to implement in hardware and are often approximated, which leads to reconstruction errors.

In [39], Unser *et al.* introduce a framework for solving continuous inverse problems that have sparse polynomial spline solutions by using the total-variation regularization. The unknown signal is assumed to be piecewise smooth and intrinsically sparse with sparsity Q , i.e. it is a nonuniform L-spline with at most Q innovations. The theorem states that the signal can be recovered from M linear measurements, where $M \geq (Q + N_0)$ and N_0 is a spline order. Papers [40]–[43] rely on the main results of the method proposed in [39] and use grid-based discretization strategies that lead to convex optimization problems.

III. BACKGROUND: SAMPLING IN SI SPACES AND INFINITE-DIMENSIONAL CS

We give a short review and the most important formulations of sampling in shift-invariant spaces and infinite-dimensional CS, which we later use to successfully combine these two methods. Excellent reviews that extensively describe sampling in SI spaces can be found in [5] and [7].

A. Sampling of Signals in Shift-Invariant Spaces

Sampling in SI spaces retains the basics of the Nyquist-Shannon theorem. An SI subspace \mathcal{A} of L_2 is spanned by the shifts of a generator $a(t)$ with period T [5], [7]. Signals in an SI subspace are expressed as weighted linear combinations of the shifts of a generator. Any signal $f(t) \in \mathcal{A}$ has the form [5]:

$$f(t) = \sum_{m \in \mathbb{Z}} d[m]a(t - mT), \quad (1)$$

where $d[m]$ are expansion coefficients that characterize the signal. The expansion coefficients $d[m]$ are not necessarily pointwise values of the signal. Shannon's theorem is a special case of SI sampling in

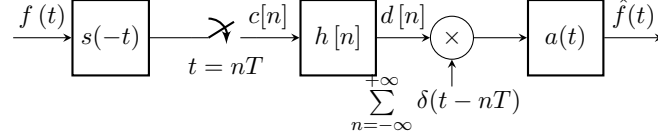


Fig. 1. Sampling and reconstruction of a signal in a shift-invariant space.

which the generator $a(t)$ corresponds to the *sinc* function. However, signals are often better represented in other SI spaces such as splines [4], [44], [45] and wavelets [3].

In order to guarantee a stable SI sampling theorem and a unique signal representation, $a(t)$ is typically chosen to form a Riesz basis [7]. A set of functions $\{a(t - mT)\}$ generate Riesz basis if it is complete and there exist two positive constants $\alpha > 0$ and $\beta < \infty$ such that [5]

$$\alpha \|\mathbf{d}\|_{\ell_2}^2 \leq \left\| \sum_{m \in \mathbb{Z}} d[m] a(t - mT) \right\|^2 \leq \beta \|\mathbf{d}\|_{\ell_2}^2, \quad (2)$$

where $\|\mathbf{d}\|_{\ell_2}^2 = \sum_m |d[m]|^2$ is the squared ℓ_2 -norm of the coefficients $d[m]$. Riesz bases provide linear independence of the basis functions and a property that a small modification of the coefficients $d[m]$ results in a small distortion of the signal [5], [7].

The SI sampling framework shares a similar sampling scheme (see Fig. 1) with the Nyquist-Shannon theorem. By analogy with antialiasing, in the SI sampling scheme the unknown signal is prefiltered by a sampling filter $s(-t)$ [5], [7]. The shifts of the sampling kernel $s(t)$ form a Riesz basis and span an SI subspace \mathcal{S} . Uniform sampling of rate $1/T$ follows the prefiltering stage. The sampling rate is determined by the number of degrees of freedom or the rate of innovation [29] of the signal, which is in an SI sampling setting dictated by the number of the expansion coefficients $d[m]$ per time unit. Samples $c[n]$ of the signal $f(t)$ defined in (1) are expressed in an SI sampling setting as:

$$c[n] = \int_{-\infty}^{\infty} f(t) s(t - nT) dt \triangleq \langle f(t), s(t - nT) \rangle, \quad (3)$$

where $\langle \cdot, \cdot \rangle$ is the conventional L_2 -inner product. The SI samples $c[n]$ in (3) are equal to

$$\begin{aligned} c[n] &= \left\langle \sum_{m \in \mathbb{Z}} d[m] a(t - mT), s(t - nT) \right\rangle \\ &= \sum_{m \in \mathbb{Z}} d[m] \langle a(t - mT), s(t - nT) \rangle \\ &= \sum_{m \in \mathbb{Z}} d[m] r_{sa}[n - m], \end{aligned} \quad (4)$$

where $r_{sa}[n] = \langle a(t), s(t - nT) \rangle$ is a sampled cross-correlation sequence between the sampling kernel $s(t)$ and the generator $a(t)$. For spline and wavelet functions $s(t)$ and $a(t)$, $r_{sa}[n]$ has only a few nonzero entries around $n = 0$, which leads to an efficient reconstruction procedure.

In order to be able to perfectly reconstruct $f(t)$ from the samples $c[n]$, the discrete-time Fourier transform (DTFT) of the sampled cross-correlation sequence, denoted by $\varphi_{SA}(e^{j\omega})$, has to satisfy a mild requirement [7]:

$$|\varphi_{SA}(e^{j\omega})| > \alpha, \quad (5)$$

for some constant $\alpha > 0$. The sequence of samples $c[n]$ in (4) have the DTFT given by

$$C(e^{j\omega}) = D(e^{j\omega})\varphi_{SA}(e^{j\omega}), \quad (6)$$

where $D(e^{j\omega})$ denotes the DTFT of the expansion coefficients $d[m]$. Consequently, a recovered sequence $\hat{d}[n]$ of the expansion coefficients is obtained by discrete-time filtering of $c[n]$ with a correction filter $h[n]$ determined by [5], [7]

$$H(e^{j\omega}) = \frac{1}{\varphi_{SA}(e^{j\omega})}. \quad (7)$$

Notice that $r_{sa}[n]$ is the Kronecker delta impulse $\delta[n]$ in the case of orthogonal and biorthogonal functions $a(t)$ and $s(t)$, thus $H(e^{j\omega}) = 1$. For example, $a(t)$ and $s(t)$ are orthogonal in the Shannon's theorem. Finally, a reconstruction $\hat{f}(t)$ of $f(t)$ is obtained by modulation of the recovered coefficients $\hat{d}[n]$ by an impulse train with period T , followed by filtering with a corresponding analog filter $a(t)$. Sampling in SI subspaces retains the basic principles of Shannon's sampling theory in which sampling and reconstruction are implemented by filtering operations.

B. Infinite-Dimensional Compressive Sensing

Basically, an inverse problem is to recover a signal f from a finite set of linear measurements $\mathbf{y} = (\mathbf{z}(f) + \mathbf{e}) \in \mathbb{R}^M$, where the noise-free measurements are given by $\mathbf{z}(f) = (\langle z_1, f \rangle, \dots, \langle z_M, f \rangle)$ and \mathbf{e} is an additive noise term that is usually assumed to be independent of the signal. Most real-world signals are continuous and the number of measurements is finite, thus the inverse problem is ill-posed. The conventional approach in order to solve such an inverse problem is to select some finite-dimensional reconstruction space \mathcal{R} spanned by $\{\psi_n\}_{n=1}^N$. By assuming that $f \in \mathcal{R}$ and denoting the expansion coefficients of f in the basis $\{\psi_n\}_{n=1}^N$ by $\mathbf{x} \in \mathbb{R}^N$, the original inverse problem can be converted to the discretized version $\mathbf{y} = \Theta\mathbf{x} + \mathbf{e}$. Matrix Θ is an $M \times N$ sensing matrix whose entries are $[\Theta_{m,n}] = \langle z_m, \psi_n \rangle$.

The compressive sensing theory [8], [9] asserts that a perfect reconstruction of the signal f from far less than N linear measurements is possible if f is Q -sparse in the finite-dimensional basis $\{\psi_n\}_{n=1}^N$, i.e.

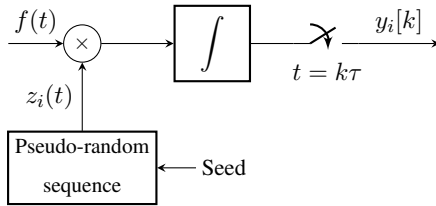


Fig. 2. Block diagram of a single channel of a bank of random demodulators.

$\|\mathbf{x}\|_{\ell_0} \leq Q \ll N$. The signal recovery is obtained by solving the constrained ℓ_1 optimization problem [46]

$$\min_{\mathbf{x} \in \mathbb{R}^N} \|\mathbf{x}\|_{\ell_1} \quad \text{subject to} \quad \|\mathbf{y} - \Theta \mathbf{x}\|_{\ell_2} \leq \kappa, \quad (8)$$

where κ is a threshold parameter determined by *a priori* estimate of an error \mathbf{e} such that $\kappa \geq \|\mathbf{e}\|_{\ell_2}$ [11]. The CS theory guarantees a faithful recovery of f from $M > 2Q$ measurements under strict conditions on Θ , namely *restricted isometry property* (RIP) and *incoherence* [9], [13], [14], [47]. The finite-dimensional setting of CS often leads to replacement of continuous measurements to its discrete counterparts, e.g. the continuous Fourier transform is replaced by its discrete analog. Modeling a continuous-domain problem in this way may easily encounter problems due to samples discrepancy [17].

In [17], Adcock and Hansen introduce an infinite-dimensional theory of CS, which addresses the problem of errors related to the inherently infinite-dimensional recovery problem. The unknown signal is a function $f : \mathbb{R} \rightarrow \mathbb{R}$ such that it has a unique expansion $f = \sum_{n=1}^{\infty} x_n \psi_n$ in a basis $\{\psi_n\}_{n=1}^{\infty}$. The measurements $\mathbf{z}(f)$ are defined as before. Assuming that the signal is sparse in the basis $\{\psi_n\}_{n=1}^{\infty}$, the reconstruction is given by

$$\min_{x \in \ell_1(\mathbb{N})} \|x\|_{\ell_1} \quad \text{s. t.} \quad \left\| \sum_{m=1}^M \left(y_m - \left\langle z_m, \sum_{n=1}^{\infty} x_n \psi_n \right\rangle \right) \right\|_{\ell_2} \leq \kappa, \quad (9)$$

which is an infinite analog to the problem in (8). The conditions on how to choose $\{z_m\}$ and discretize the infinite-dimensional sensing matrix to guarantee recovery of the expansion coefficients up to a certain scale are derived in [17].

IV. RD-BASED MEASUREMENT MODEL FOR SIGNALS IN SI SPACES

We propose an acquisition system consisting of a bank of random demodulators [32], [34] as a hardware front-end. Conventionally, in the i -th RD channel (see Fig. 2), a bandlimited signal $f(t)$ is multiplied by a continuous-time demodulating signal $z_i(t)$ created from a pseudo-random chipping sequence of ± 1 . That is, $z_i(t)$ switches between the levels ± 1 at least at the Nyquist rate of the signal $f(t)$. The demodulated

signal is integrated prior to being sampled at a low rate $1/\tau$. The integrator is being reset after each sample $y_i[k]$ is taken.

In this paper, we consider signals that lie in a more general class of shift-invariant spaces. We assume that an input signal $f(t)$, in an SI subspace \mathcal{A} of L_2 , is spanned by a single generator $a(t)$. The signal is given by (1) with a rate of innovation $\rho = 1/T$. The signal is multiplied by a continuous-time signal $z_i(t)$ that switches between levels ± 1 at the rate of innovation ρ . Let us define the box function also known as B-spline of degree 0:

$$b^0(t) = \begin{cases} 1, & 0 < t \leq 1 \\ 0, & \text{otherwise} \end{cases}, \quad (10)$$

which satisfies (2). In fact, the basis functions $\{b^0(t-n)\}$ are orthonormal, i.e. the constants $\alpha = \beta = 1$. If we define a sampling kernel $s(t) = b^0(t/T)$, where $1/T$ is the switching rate of $z_i(t)$, then the shifts of the sampling kernel $\{s(t-nT)\}$ span an SI subspace \mathcal{S} . The demodulating signal $z_i(t)$ is a signal that lie in the SI subspace \mathcal{S} and is given by

$$z_i(t) = \sum_{n=1}^N \phi_i[n] \sum_{k \in \mathbb{Z}} s(t-nT-kNT), \quad (11)$$

where $\phi_i[n]$ are expansion coefficients of ± 1 values. Without loss of generality, in the proposed setting we set demodulating functions to be periodic with a period $\tau = NT$ and $\phi_i[n]$ are cyclically repeated. The demodulated signal $f(t) \cdot z_i(t)$ is integrated and subsequently sampled at a low rate $1/\tau$ to obtain a sequence of measurements $\{y_i[k]\}$.

A single measurement in the i -th channel of the acquisition system is given by:

$$y_i[k] = \int_{k\tau}^{(k+1)\tau} f(t)z_i(t)dt, \quad (12)$$

where k denotes an integration interval. By applying (1) and (11), (12) is expanded to:

$$y_i[k] = \sum_{n=1}^N \phi_i[n] \sum_{m \in \mathbb{Z}} d[m] \int_{k\tau}^{(k+1)\tau} a(t-mT)s(t-nT-k\tau)dt. \quad (13)$$

Since the integration interval covers the whole support of exactly N basis functions of the SI subspace \mathcal{S} , the integration result in (13) for given k , n and m is equal to the sampled cross-correlation sequence

$$r_{sa}[n+kN-m] = \langle a(t-mT), s(t-nT-k\tau) \rangle. \quad (14)$$

By using (14), we can discretize the continuous-domain measurement process in an exact way. Thus, (13) is given in a discrete form by

$$y_i[k] = \sum_{n=1}^N \phi_i[n] \sum_{m \in \mathbb{Z}} d[m] r_{sa}[n+kN-m], \quad (15)$$

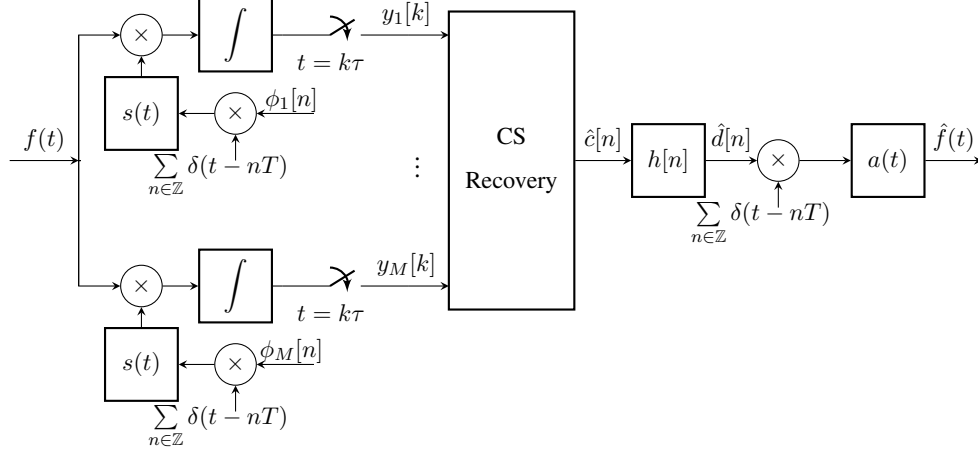


Fig. 3. Block diagram of a system for compressive sensing of signals in shift-invariant subspaces with a sampling kernel $s(t)$ and a correction filter $h[n]$.

which, by applying (4), becomes simply

$$y_i[k] = \sum_{n=1}^N \phi_i[n] c_k[n]. \quad (16)$$

Here, $c_k[n]$ represents the conventional samples in an SI sampling setting corresponding to the k -th integration interval. Using this strategy, low-rate measurements $\{y_i[k]\}$ are weighted linear combinations of the SI samples $c_k[n]$.

The system's front-end consists of M channels with various demodulating functions $\{z_i(t)\}_{i=1}^M \in \mathcal{S}$, where $M < N$. In each channel, the demodulated signal is integrated and sampled at a rate $1/\tau$, which leads to a system with a sampling rate $M/\tau = M/(NT)$. The proposed system allows for sampling of signals with a much lower sampling rate in contrast to the conventional high-rate method described in Section III-A. The front-end of the proposed system is illustrated on the left hand side of the block diagram in Fig. 3. The chipping sequence in the RD scheme is replaced by an analog filter $s(t)$ that is a box function in this particular case. The input to the filter $s(t)$ is a modulated impulse train $\sum_n \phi_i[n] \delta(t - nT)$.

The measurement procedure of the system with additive noise is given in a matrix form by

$$\begin{bmatrix} y_1[k] \\ \vdots \\ y_M[k] \end{bmatrix} = \begin{bmatrix} \phi_1[1] & \cdots & \phi_1[N] \\ \vdots & \vdots & \vdots \\ \phi_M[1] & \cdots & \phi_M[N] \end{bmatrix} \cdot \begin{bmatrix} c_k[1] \\ \vdots \\ c_k[N] \end{bmatrix} + \mathbf{e}_k \quad (17)$$

or

$$\mathbf{y}_k = \mathbf{\Phi} \mathbf{c}_k + \mathbf{e}_k, \quad (18)$$

where Φ is an $M \times N$ measurement matrix consisting of ± 1 values and $\mathbf{e}_k \in \mathbb{R}^M$ is an unknown error term. Furthermore, \mathbf{y}_k and \mathbf{c}_k are vectors of the measurements and SI samples, respectively. Since $M < N$, the proposed finite-dimensional inverse problem is underdetermined. In the next section, we show how to recover the SI samples from an underdetermined set of equations by using the CS reconstruction procedure.

V. RECONSTRUCTION OF SIGNALS IN SI SPACES FROM RD MEASUREMENTS

The objective is to recover SI samples \mathbf{c}_k from a reduced set of linear measurements \mathbf{y}_k . In order to be able to recover the SI samples by exploiting the CS theory, the samples have to be sparse in the time or a transform domain. The vast majority of works, such as [29], [37], [39], assume that an analog signal in an SI subspace is sparse in the time domain, i.e. the signal is characterized by only a few nonzero expansion coefficients $d[m]$. Analogously, we could have assumed that the SI samples \mathbf{c}_k in the proposed measurement model are sparse in the time domain for signals that are spanned by a generator with a narrow support. Instead, in this paper, we treat the case in which the SI samples \mathbf{c}_k , and in the sequel the expansion coefficients $d[m]$, are sparse in a certain representation basis Ψ . Thus, the SI samples can be represented as $\mathbf{c}_k = \sum_{l=1}^N x_k[l] \psi_l$, where $\{x_k[l]\}_{l=1}^N = \mathbf{x}_k$ is a set of expansion coefficients and ψ_l are columns of $\Psi \in \mathbb{R}^{N \times N}$. The inverse problem in (18) is then given by

$$\mathbf{y}_k = \Phi \Psi \mathbf{x}_k + \mathbf{e}_k = \Theta \mathbf{x}_k + \mathbf{e}_k, \quad (19)$$

where Θ is an $M \times N$ sensing matrix. CS is concerned with the RIP [8], [13], [47] which, similarly to the condition in (2), secures that the sensing matrix Θ preserves the geometry of the sparse vectors \mathbf{x} . Additionally, Θ should be made of a low coherent pair (Φ, Ψ) of a measurement and a representation matrix to allow for a high subsampling [10]. A combination of a measurement matrix built using random entries from a certain probability distribution and any fixed representation basis has the RIP with a high probability [48]. Moreover, the pair of a random matrix and any fixed representation basis is largely incoherent, which makes random matrix a good choice for the measurement matrix in a CS setup [8], [10]. For a sensing matrix that satisfies the RIP and incoherence property, CS guarantees a perfect recovery of a Q -sparse signal from $M \geq 2Q$ measurements with high probability.

Real-world signals are rarely truly sparse, but rather asymptotically sparse [12], [49]. That is, the vectors \mathbf{x} of expansion coefficients have a lot of small coefficients, but only a few true zeros if any, and the signals have a structure of being far sparser at fine scales (or high frequencies) than at coarse scales. A refined theory of CS [12], [49] offers generalized principles of incoherence and uniform random sampling, and avoids the RIP, which may be too strong an assumption in practice. The theory introduces

asymptotic incoherence and sparsity, and multilevel sampling [12], [49], [50] instead of universal random subsampling. Briefly, a sensing matrix Θ is asymptotically incoherent if the first few rows or columns of the matrix are large and values get asymptotically smaller as we move away from this region. Fourier/wavelet and Hadamard/wavelet transform matrices are examples of asymptotically incoherent pairs because of a high correlation of low-order frequencies and scales, and a decrease in the correlation as frequencies get higher and scales become finer. Asymptotic incoherence and sparsity structure lead to a multilevel sampling. That is, we should fully sample high coherence rows where important information about the signal is likely to be contained and as coherence starts to decrease, we can subsample gradually. The sparsity structure of the signal is exploited by using multilevel sampling of asymptotically incoherent matrices, which leads to better reconstructions than the universal subsampling with random measurement matrices [12], [49].

In this paper, we assume that the SI samples are asymptotically sparse in a representation basis such as the discrete Fourier (DFT), cosine (DCT) and wavelet transform (DWT). Consequently, we use the multilevel sampling strategy with asymptotically incoherent matrices. We propose the use of measurement matrices with only ± 1 values in order to maintain the low complexity of the multiplier design. The Walsh-Hadamard transform (WHT) matrix, which is an example of a generalized class of Fourier transforms, fits the proposed setup and its row entries are used as expansion coefficients $\phi_i[n]$ of a demodulating function $z_i(t)$. The signal is recovered from such measurements by using ℓ_1 minimization algorithms [46], [51]. We recover the SI samples by solving the *Quadratically-Constrained Basis Pursuit* (QCBP) optimization program:

$$\min_{\mathbf{x}_k \in \mathbb{R}^N} \|\mathbf{x}_k\|_{\ell_1} \quad \text{s. t.} \quad \|\mathbf{y}_k - \Theta \mathbf{x}_k\|_{\ell_2} \leq \kappa, \quad (20)$$

where $\kappa \geq \|\mathbf{e}_k\|_{\ell_2}$. In practice, \mathbf{e}_k is often unlikely to be known. Despite that, the QCBP shows to be quite robust even when the error is underestimated [52].

A recovered set $\{\hat{\mathbf{c}}_k\}$ of the SI samples $\{\mathbf{c}_k\}$ is further used to reconstruct the signal in the conventional way for the SI sampling setting described in Section III-A. The recovered SI samples $\{\hat{\mathbf{c}}_k\}_{k=1}^K$ in K intervals of length N are arranged into a sequence $\hat{\mathbf{c}}[n]$ and filtered by the correction filter given in (7) to obtain expansion coefficients $\hat{d}[n]$ of a signal $\hat{f}(t) \in \mathcal{A}$. The obtained expansion coefficients $\hat{d}[n]$ are modulated by an impulse train with period T and filtered by the corresponding analog filter $a(t)$. The reconstruction scheme is illustrated on the right hand side of a block diagram in Fig. 3.

Even though, theoretically, various functions belong to the class of SI spaces, the correction filter $H(e^{j\omega})$ may be difficult to implement in practice. There are numerous filter design techniques that can be used to closely approximate the desired response of $H(e^{j\omega})$ with a finite impulse response (FIR) or

an infinite impulse response (IIR) filter. However, in case when the generator $a(t)$ is a B-spline, $H(e^{j\omega})$ can be determined analytically [5]. The filter is then a non-causal IIR filter with a few coefficients corresponding to values of the cross-correlation sequence $r_{sa}[n]$. The filter can be decomposed into a causal and an anti-causal part, which leads to a forward\backward filtering [44], [45] of recovered SI samples. Alternatively, as an impulse response of the IIR filter has a fast decay, it can be approximated by a FIR filter allowing for a continuous filtering of the SI samples with a short delay.

VI. GENERALIZATION OF THE PROPOSED METHOD TO OTHER SAMPLING KERNELS

Physical devices often impose the sampling operator, leaving limited freedom to design the sampling strategy. That is, the sampling kernel is not always possible to be the box function proposed in Section IV. Furthermore, multiplication by the ± 1 chipping sequence is a bottleneck of the RD-based system caused by the settling times of inverters and multiplexers. Instant change of the sign in analog parts is not realizable by real components and should be avoided when possible. For example, a better choice would be multiplication by a continuous function that has linear transition between different levels. Such functions lie in a subspace of B-splines of order 1. Thus, we propose a generalization of the framework proposed in the previous sections, which adopts the system to arbitrary sampling kernels.

A single measurement in the i -th channel of the proposed acquisition system is given in (12), where $f(t)$ denotes an input signal in an SI subspace \mathcal{A} , k denotes an integration interval of duration $\tau = NT$ and $z_i(t)$ is a demodulating signal lying in an SI subspace \mathcal{S} . Here, \mathcal{S} is spanned by the sampling kernel shifts $\{s(t - nT)\}$ which are not necessarily the shifts of the box function. The measurement is given by

$$y_i[k] = \sum_{n \in \mathbb{Z}} \phi_i[n] \sum_{m \in \mathbb{Z}} d[m] \int_{k\tau}^{(k+1)\tau} a(t - mT) s(t - nT) dt. \quad (21)$$

Since $s(t)$ is an arbitrary sampling kernel, the basis functions may overlap each other. Thus, in general, we must include cases in which the integration interval covers more than exactly N basis functions of the SI subspace \mathcal{S} . It follows that the integration results in (21) can not be substituted simply by the cross-correlation sequence as in Section IV, but they can be written in an infinite matrix \mathbf{R}_k with rows and columns corresponding to n and m , respectively. The matrix \mathbf{R}_k is mainly filled with zeros except for a few entries around the diagonal for values of n and m close to kN . The continuous-domain measurement process can be discretized in an exact way and is given in a discrete form by

$$y_i[k] = \sum_{n \in \mathbb{Z}} \phi_i[n] \sum_{m \in \mathbb{Z}} d[m] R_{n,m}^k, \quad (22)$$

where $R_{n,m}^k$ is an entry of \mathbf{R}_k for given n and m . For $s(t)$ and $a(t)$ of finite support, the nonzero values in \mathbf{R}_k can be concisely written in a submatrix $\tilde{\mathbf{R}}$ of finite dimensions which is universal for all integration

intervals denoted by k . For spline and wavelet generators, $\tilde{\mathbf{R}}$ is particularly easy to implement. In RD-based measurement settings, the matrix $\tilde{\mathbf{R}}$ is a rectangular matrix with a cross-correlation sequence $r_{sa}[n]$ on its diagonal. A special case occurs when both $s(t)$ and $a(t)$ are B-splines of degree 0, then $\tilde{\mathbf{R}}$ is an $N \times N$ identity matrix. An example of the matrix $\tilde{\mathbf{R}}$, when both $s(t)$ and $a(t)$ are B-splines of degree 1, is given in Appendix A.

By applying $\tilde{\mathbf{R}} \in \mathbb{R}^{H \times L}$, the measurement becomes

$$y_i[k] = \phi_{i,k} \tilde{\mathbf{R}} \mathbf{d}_k, \quad (23)$$

where $\phi_{i,k} \in \mathbb{R}^H$ is a row vector of the expansion coefficients corresponding to the sampling basis functions whose support is included in the k -th integration interval. Equivalently, $\mathbf{d}_k \in \mathbb{R}^L$ is a vector of the expansion coefficients corresponding to signal basis functions whose support is included in the k -th integration interval. The system's front-end consists of $M < N$ channels. The demodulated signal is integrated and sampled at rate $1/\tau$, leading to a system with a sampling rate $M/\tau = M/(NT)$. The front-end of the system is illustrated on the left hand side of the block diagram in Fig. 3. Contrarily to the setting in Section IV, the sampling kernel $s(t)$ is an arbitrary generator of an SI subspace.

The measurement procedure of the system corrupted by noise \mathbf{e}_k is given by

$$\mathbf{y}_k = \Phi_k \tilde{\mathbf{R}} \mathbf{d}_k + \mathbf{e}_k, \quad (24)$$

where Φ_k is a measurement matrix with rows $\{\phi_{i,k}\}_{i=1}^M$. The proposed system of equations is under-determined. In order to recover the expansion coefficients \mathbf{d}_k , we induce the sparsity and use the CS reconstruction technique. We can assume that the signal is sparse in the time domain, i.e. the vector of expansion coefficients \mathbf{d}_k has only a few nonzero entries. Such an assumption is exploited in [39]–[43] where the observed signals lie in the L-spline and B-spline spaces. However, in this paper, we assume the expansion coefficients \mathbf{d}_k are sparse in a certain transform domain $\Psi \in \mathbb{R}^{L \times L}$. The expansion coefficients are represented as $\mathbf{d}_k = \Psi \mathbf{x}_k$, where $\mathbf{x}_k \in \mathbb{R}^L$ is the sparse vector of coefficients in the transform domain. The problem in (24) is written as

$$\mathbf{y}_k = \Phi_k \tilde{\mathbf{R}} \Psi \mathbf{x}_k + \mathbf{e}_k = \Theta \mathbf{x}_k + \mathbf{e}_k, \quad (25)$$

where $\Theta = \Phi_k \tilde{\mathbf{R}} \Psi$ is a sensing matrix.

Compressive sensing is concerned with a low coherent pair of measurement and representation matrices. Since we introduced the matrix $\tilde{\mathbf{R}}$ into the inverse problem, the coherence between Φ_k , $\tilde{\mathbf{R}}$, and Ψ should be addressed. Clearly, $\tilde{\mathbf{R}}$ affects the coherence of the conventional (Φ, Ψ) -pair and its recovery ability.

The recovery ability is related to *coherence* which measures the maximal correlation between the two matrices:

$$\mu(\Phi, \Psi) \triangleq \max_{\substack{1 \leq i \leq M \\ 1 \leq j \leq N}} \frac{|\phi_i \psi_j|}{\|\phi_i\|_{\ell_2} \|\psi_j\|_{\ell_2}}, \quad (26)$$

where $\{\phi_i\}$ and $\{\psi_j\}$ are rows and columns of Φ and Ψ , respectively. The coherence should be as small as possible, as the minimal number of measurements for perfect reconstruction of Q -sparse signals depends on this property. In the proposed generalized method, the coherence can be measured in two ways by joining the matrices Φ_k and $\tilde{\mathbf{R}}$ or $\tilde{\mathbf{R}}$ and Ψ , namely by calculating $\mu(\Phi_k \tilde{\mathbf{R}}, \Psi)$ or $\mu(\Phi_k, \tilde{\mathbf{R}} \Psi)$. Traditionally, random matrices are largely incoherent with any representation matrix [8] and the same is expected for $(\Phi_k, \tilde{\mathbf{R}} \Psi)$ -pairs, where $\tilde{\mathbf{R}} \Psi$ can be seen as a representation matrix. However, a more proper way to compute the coherence is to join Φ_k and $\tilde{\mathbf{R}}$ and calculate $\mu(\Phi_k \tilde{\mathbf{R}}, \Psi)$, since the expansion coefficients are assumed to be sparse in the representation matrix Ψ and $\tilde{\mathbf{R}}$ is based on the measurement setup and signal subspace. A new measurement matrix $\Phi_k \tilde{\mathbf{R}}$ largely depends on the relation between a signal generator and a sampling kernel, which may introduce a deterministic structure and consequently affect the coherence with a representation matrix. However, in many cases a random matrix is an adequate choice for the measurement matrix Φ_k , which leads to a perfect recovery of a Q -sparse signal with a high probability.

A more convenient way of analyzing the reconstruction ability of the matrix Θ is the *mutual coherence* that measures the maximal correlation between columns of Θ . The mutual coherence of Θ is defined as

$$\mu\{\Theta\} \triangleq \max_{\substack{1 \leq i, j \leq L \\ i \neq j}} \frac{|\theta_i^T \theta_j|}{\|\theta_i\|_{\ell_2} \|\theta_j\|_{\ell_2}}, \quad (27)$$

where θ_i is a column of Θ and L is the number of columns in Θ . Small values of the mutual coherence are required as they enable CS recovery of signals with denser representations.

For deterministic measurement matrix, e.g. the WHT, the sensing matrix Θ keeps the asymptotic incoherence property [12], [49] from Section V. That is, one should use the multilevel subsampling strategy [50] in order to exploit asymptotic incoherence and sparsity.

The expansion coefficients are recovered by solving the QCBP optimization program:

$$\min_{\mathbf{x}_k \in \mathbb{R}^L} \|\mathbf{x}_k\|_{\ell_1} \quad \text{s. t.} \quad \|\mathbf{y}_k - \Theta \mathbf{x}_k\|_{\ell_2} \leq \kappa, \quad (28)$$

where $\kappa \geq \|\mathbf{e}_k\|_{\ell_2}$. The vector of coefficients $\mathbf{x}_k \in \mathbb{R}^L$, where $L \geq N$, is used to obtain the expansion coefficients $\hat{\mathbf{d}}_k \in \mathbb{R}^L$. The number of recovered coefficients is equal to the number of coefficients N corresponding to the k -th integration interval plus the $L - N$ coefficients that correspond to the neighboring intervals. Next, we concatenate the expansion coefficients $\{\hat{\mathbf{d}}_k\}_{k=1}^K$ obtained in K intervals

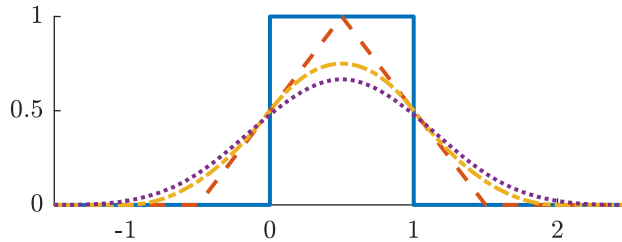


Fig. 4. B-spline basis functions of degrees $p = 0$ to 3. As p increases, the basis functions flatten out and their support expands.

of length $\tau = NT$. We apply the weighted average to the expansion coefficients on the boundaries of the integration intervals which appear in two consecutive vectors $\hat{\mathbf{d}}_k$. The weights are determined by the amount of area under a basis function in the observed integration interval. An example of the concatenation for expansion coefficients of B-splines of order 1 is given in Appendix B. The concatenated expansion coefficients $\hat{d}[n]$ are modulated by an impulse train with period T and filtered by the corresponding analog filter $a(t)$ in order to reconstruct the signal $f(t)$. The reconstruction scheme is similar to the one in Fig. 3, but without a correction filter $h[n]$, which is here embedded in the CS reconstruction procedure.

VII. NUMERICAL EXPERIMENTS

We validate the proposed system based on simulations conducted on signals that are synthetically made Q -sparse and real-world signals that can be seen as asymptotically sparse. All the simulations were performed in the programming language MATLAB and the ℓ_1 optimization programs were solved using SPAMS v2.6 optimization toolbox [53].

A. Q -Sparse Signals

In order to prove that the proposed framework perfectly reconstructs observed signals in an SI subspace under the sparsity assumption, we synthetically induced sparsity in a real-world audio signal which was previously interpolated by continuous B-spline basis functions of various degrees.

1) *Test Signals:* A test signal is of the form

$$f(t) = \sum_{m \in \mathbb{Z}} d[m]a(t - mT), \quad (29)$$

where $a(t)$ is a generator whose shifts span a B-spline subspace \mathcal{A} of degree p . For simplicity, we set the period $T = 1$. Fig. 4 illustrates the generators of the B-spline subspaces. The signal is divided in intervals of length $\tau = NT = 1024$ so that $\mathbf{d}_k \in \mathbb{R}^N$ is a vector of expansion coefficients associated with the k -th interval. The audio signal is of finite length and the number of intervals is $K = 71$. The expansion

coefficients $\{\mathbf{d}_k\}_{k=1}^K$ are synthetically made Q -sparse in the DCT domain. We select the sparsity ratio $q = Q/N$ to 10%, 15% and 20%, which correspond to Q : 102, 154 and 205 nonzero entries, respectively.

2) *Measurements:*

- **RD-based measurement:** This case simulates the measurement procedure of a parallel version of the RD, which is described in detail in Section IV. Demodulating signals $\{z_i(t)\}_{i=1}^M$, where $M < N$, lie in the B-spline subspace of degree 0, i.e. the sampling kernel $s(t)$ is a box function $b^0(t)$ (10). Expansion coefficients $\{\phi_i[n]\}$ of $\{z_i(t)\}$ are i.i.d. random values of ± 1 s, which cyclically repeat with period $N = 1024$. The expansion coefficients $\{\phi_i[n]\}$ form a measurement matrix $\Phi \in \mathbb{R}^{M \times N}$. Sampling rate in a single channel is N times lower than the rate of innovation $\rho = 1/T = 1$ of the signals. Vector of measurements $\mathbf{y}_k \in \mathbf{R}^M$, that is obtained at the end of an interval k , is a weighted linear combination of the SI samples contained in a vector $\mathbf{c}_k \in \mathbb{R}^N$. The measurement procedure is given by $\mathbf{y}_k = \Phi \mathbf{c}_k + \mathbf{e}_k$, where \mathbf{e}_k is an error term.
- **Measurement with an arbitrary sampling kernel $s(t)$:** Here, measurements are obtained by simulating the measurement procedure of a generalized parallel RD, in which the sampling kernel $s(t)$ lies in an arbitrary SI subspace (see Section VI). In our settings, demodulating signals $\{z_i(t)\}_{i=1}^M$, where $M < N$, lie in a B-spline subspace of degree p , for $p = 0, 1$ or 2 . The expansion coefficients $\{\phi_i[n]\}$ and the sampling rate are the same as those in the previous measurement case. The expansion coefficients $\{\phi_i[n]\}$ construct a measurement matrix $\Phi_k \in \mathbb{R}^{M \times H}$, where $H \geq N$. The relation between $a(t)$ and $s(t)$ in a single integration interval is contained in a matrix $\tilde{\mathbf{R}}$. Thus, a vector of measurements $\mathbf{y}_k \in \mathbf{R}^M$ is related to the expansion coefficients $\mathbf{d}_k \in \mathbb{R}^L$ by expression $\mathbf{y}_k = \Phi_k \tilde{\mathbf{R}} \mathbf{d}_k + \mathbf{e}_k$.

3) *Reconstruction:*

- **CS recovery followed by a discrete-time filter $h[n]$:** We use this type of reconstruction exclusively for measurements acquired by the parallel RD with piecewise constant demodulating signals (see Section V). The SI samples \mathbf{c}_k , which are assumed sparse in the DCT domain, are recovered by solving the optimization problem (20). The random measurement matrix Φ leads to the sensing matrix Θ that has nice CS properties. The threshold parameter κ should be tuned according to the measurement error and to the type of a generator $a(t)$. Furthermore, when the generator $a(t) = s(t) = b^0(t)$, SI samples are equal to the expansion coefficients \mathbf{d}_k , due to the orthonormality of the basis functions. Thus, the SI samples \mathbf{c}_k are ideally Q -sparse in the DCT domain. However, the equality $\mathbf{c}_k = \mathbf{d}_k$ does not hold for other choices of the generator $a(t)$. Consequently, the recovered SI samples $\hat{\mathbf{c}}_k$ are arranged into a sequence $\hat{c}[n]$ and are filtered by a discrete-time correction filter

TABLE I
CORRECTION FILTERS FOR B-SPLINE GENERATORS OF DEGREE p

p	0	1	2	3
$H(z)$	1	$\frac{8}{z+6+z^{-1}}$	$\frac{6}{z+4+z^{-1}}$	$\frac{384}{z^2+76z+230+76z^{-1}+z^{-2}}$

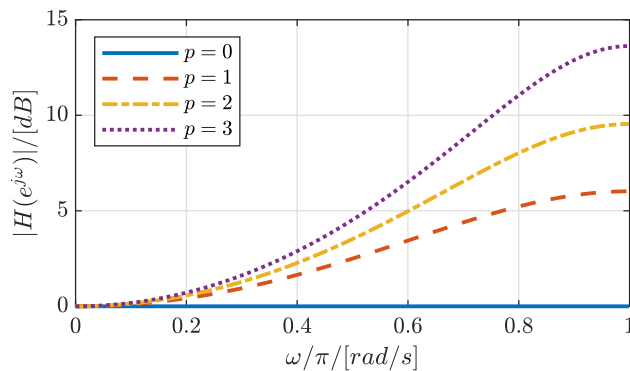


Fig. 5. Magnitudes of the frequency responses of the discrete-time correction filters given in Table I.

$h[n]$ in order to obtain the expansion coefficients \mathbf{d}_k , which characterize the signal in the subspace \mathcal{A} . Correction filters for various B-spline generators $a(t)$ are given in Table I. The correction filters are symmetric and stable, i.e. the poles are reciprocal and do not lie on the unit circle [44]. Fig. 5 shows the frequency responses of the correction filter $H(z)$ for various degrees p of the B-spline generator $a(t)$.

- CS recovery with an embedded discrete-time filter:** This reconstruction procedure is a generalization of the RD-based measurement and recovery to arbitrary sampling kernels. We recover \mathbf{d}_k by solving the ℓ_1 -minimization problem (28). The sensing matrix Θ consists of three matrices, namely the random measurement matrix Φ_k , the correlation matrix $\tilde{\mathbf{R}}$, and the DCT matrix Ψ . The correlation matrix $\tilde{\mathbf{R}}$ contains the cross-correlation sequence $r_{sa}[n]$ on its diagonal, which is an inverse FIR filter of $H(z)$ in a matrix form. The reconstruction ability of Θ can be measured by the coherence (26) and mutual coherence (27). The coherence $\mu(\Phi_k, \tilde{\mathbf{R}}, \Psi)$ is comparable to the coherence of the traditional (Φ, Ψ) -pair for the same random sequences $\{\phi_i[n]\}$ and representation matrix Ψ , and slightly increases as the degrees of the B-spline generator $a(t)$ and sampling kernel $s(t)$ increase. However, it is sufficiently low to achieve a perfect recovery for a universal random measurement matrix Φ_k . Finally, the threshold parameter κ in (28) is tuned according to the measurement error.

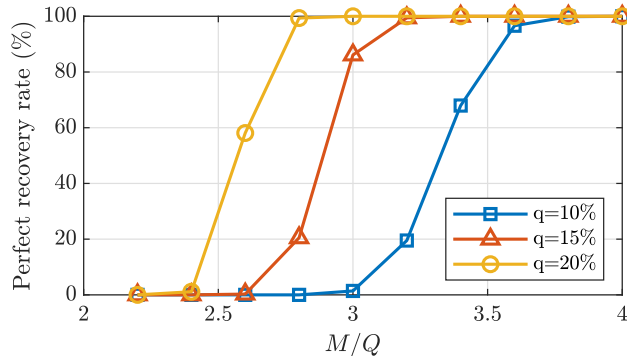


Fig. 6. **RD-based measurements and CS recovery followed by a correction filter.** Perfect recovery rates of a Q -sparse signal in the B-spline space of degree 0 for various number of measurements M and sparsity ratios q .

4) *Experimental Results:* We simulated every setting 20 times in order to obtain reliable results. We selected 20 sets of $\{\phi_i[n]\}_{i=1}^N$, for $n = 0, \dots, N-1$, that are i.i.d. random values of ± 1 s. These expansion coefficients of the demodulating signals, which are periodic with NT , were used in the simulations for all of the proposed settings. Since the test signals had been made synthetically Q -sparse, we were able to calculate the perfect recovery rate for various number of measurements M . Signal-to-noise ratio (SNR) assesses the quality of reconstructions, where the reconstruction error is treated as noise. We considered SNR of ≥ 70 decibels to be the perfect reconstruction, due to the numerical errors. In noise-corrupted measurements, the additive noise term was modeled by white Gaussian noise with variance σ_n^2 . The standard deviation σ_n was set to 5% and 10% of the measurement vector's standard deviation σ_y .

- **RD-based experiments:** In this case, we used the RD-based measurements and the CS recovery followed by a discrete-time filter $h[n]$. Since the SI samples are ideally Q -sparse only for a B-spline generator $a(t)$ of degree 0, we calculated perfect recovery rates for this setting using various number of measurements M and sparsity ratios q of the test signal (see Fig. 6). This setting can be seen as the traditional CS problem and the simplest of the proposed settings. The graph shows that in all simulations, more than 99% of the intervals are perfectly recovered for M/Q ratios: 3.8, 3.2 and 2.8, which are associated to sparsity ratios 10%, 15% and 20%, respectively. The M/Q ratios correspond to number of measurements M : 388 ($q = 10\%$), 490 ($q = 15\%$) and 571 ($q = 20\%$). The same numbers of measurements were subsequently used in the assessment of the reconstruction results for other settings.

Reconstruction results of the proposed framework for B-spline generators $a(t)$ of degree $p = 0, \dots, 3$ and various sparsity ratios are given in Table II. The reconstruction quality is the highest for noiseless settings with B-spline generator $a(t)$ of degree 0, clearly because of the sparsity property.

TABLE II
RECONSTRUCTION QUALITY IN TERMS OF SNR IN DECIBELS FOR Q -SPARSE SIGNALS AND RD-BASED MEASUREMENTS

σ_n	$q=10\%$			$q=15\%$			$q=20\%$		
	0	$\frac{\sigma_y}{20}$	$\frac{\sigma_y}{10}$	0	$\frac{\sigma_y}{20}$	$\frac{\sigma_y}{10}$	0	$\frac{\sigma_y}{20}$	$\frac{\sigma_y}{10}$
B_0	83.93	17.34	12.36	75.72	16.61	12.30	82.17	16.11	12.36
B_1	40.69	17.16	12.34	39.82	16.56	12.39	41.17	16.28	12.56
B_2	37.33	17.34	12.59	38.39	16.82	12.66	37.19	16.53	12.74
B_3	34.92	17.65	13.13	35.88	17.31	13.16	34.54	17.02	13.14

However, even though the SI samples are not ideally Q -sparse in the DCT domain for B-spline generators $a(t)$ of degree 1, 2 and 3, the framework has shown to be efficient in these cases, too. In noiseless experiments, reconstruction quality deteriorates as the degree of the B-spline generators $a(t)$ increases. This is mainly due to the relation of the SI samples \mathbf{c}_k and the expansion coefficients \mathbf{d}_k , which are more similar for lower degrees of B-splines. Additionally, the correction filters progressively amplify high-frequency components as the degree of the B-spline generator increases. This results in an amplification of the reconstruction error, which is more of the high-frequency nature, and consequently deteriorates the reconstruction quality. For noise-corrupted measurements, the framework achieves similar or slightly better reconstruction results than the simplest setting which is related to the traditional CS.

- Experiments based on the generalized method:** Here, we used the measurements obtained by the generalized acquisition method and the CS recovery with an embedded discrete-time filter. First, we calculated the perfect recovery rates for settings where the B-spline generators $a(t)$ are of degree 0, \dots , 3 and sampling kernels $s(t)$ are of degree 0, 1 and 2 (see Fig. 7). The sparsity ratio q is set to 15%. Notice that the perfect recovery rate of a signal in B-spline subspace of degree 0 in Fig. 7a matches the rate of a signal with sparsity ratio $q = 15\%$ in Fig. 6, since these two inverse problems are equal. The generalized method offers a perfect reconstruction of expansion coefficients by using random measurement matrices Φ_k . It can be seen that the minimal M for a perfect recovery is smaller than in the traditional problem of (Φ, Ψ) -pair for $a(t) = b^1(t)$ and $a(t) = b^2(t)$ in Fig. 7a, $a(t) = b^0(t)$ and $a(t) = b^1(t)$ in Fig. 7b and Fig. 7c. However, as the degree of B-spline basis functions $a(t)$ and $s(t)$ increases, the growth of the coherence negatively affects the minimal number of measurements M that is needed for a perfect recovery.

In order to compare reconstruction results with the ones in Table II, we set sparsity ratio q to

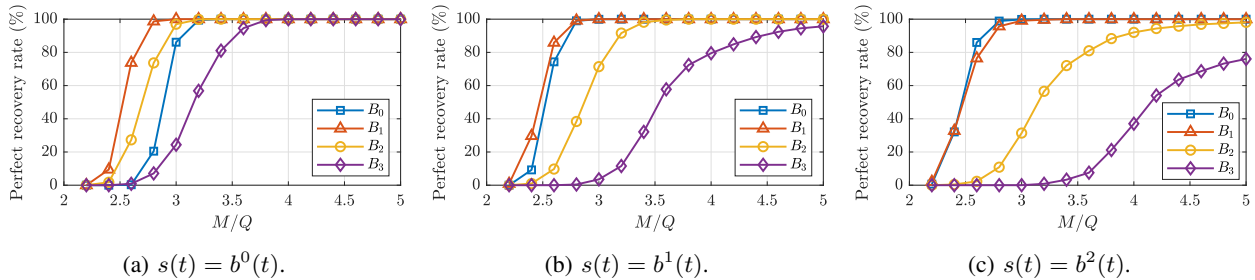


Fig. 7. **Generalized reconstruction method with arbitrary sampling kernels.** Perfect recovery rates of a Q -sparse signal in the B-spline space of degree $p = 0, \dots, 3$ for various number of measurements M . The sampling kernel $s(t)$ is a B-spline basis function of degree: (a) 0, (b) 1 and (c) 2.

TABLE III

RECONSTRUCTION QUALITY IN TERMS OF SNR IN DECIBELS FOR Q -SPARSE SIGNALS ($q = 15\%$) AND MEASUREMENTS WITH VARIOUS SAMPLING KERNELS

σ_n	$s(t)=b^0(t)$			$s(t)=b^1(t)$			$s(t)=b^2(t)$		
	0	$\frac{\sigma_y}{20}$	$\frac{\sigma_y}{10}$	0	$\frac{\sigma_y}{20}$	$\frac{\sigma_y}{10}$	0	$\frac{\sigma_y}{20}$	$\frac{\sigma_y}{10}$
B_0	75.72	16.61	12.30	85.52	19.00	13.82	84.37	18.95	13.98
B_1	86.28	19.96	14.74	85.61	20.08	15.00	83.73	19.82	14.99
B_2	82.31	19.03	14.59	48.08	18.46	14.50	31.60	17.99	14.34
B_3	28.00	17.69	14.32	23.06	17.33	14.20	21.41	17.10	14.10

15% and the ratio M/Q to 3.2. Table III shows SNRs of the reconstructions for various degrees of the B-spline generators and sampling kernels. In noiseless experiments, while the number of measurements is large enough for a perfect recovery, the generalized method achieves much better results than the previous one. However, when the degrees of B-spline basis functions $a(t)$ and $s(t)$ increase, the reconstruction quality decreases below the reconstruction quality of the method with a correction filter, due to the higher coherence between the $(\Phi\tilde{\mathbf{R}}, \Psi)$ -pair than between the (Φ, Ψ) -pair. For noise-corrupted measurements, the B-spline generator $a(t)$ of degree 1 achieves better reconstruction results than the other generators. Furthermore, the generalized method achieves better results than the method with a correction filter in all noise-corrupted experiments. This is due to the frequency responses of the correction filter $H(z)$ and its inverse filter. While $H(z)$ amplifies reconstruction error after the CS recovery in the framework with a discrete-time correction filter, its inverse filter is lowpass and is embedded in the CS recovery of the generalized method.

B. Real-World Signals

Simulations for real-world signals were conducted on publicly available free samples of a high-resolution audio [54]. The original audio signal was sampled at the rate of 192 kHz. The signal is asymptotically sparse in the Fourier basis with large coefficients corresponding to low-order frequencies and a lot of small coefficients, but only a few true zeros.

We simulated the measurement procedure described in Sections IV and VI with B-spline sampling kernels of order 0, 1 and 2. In order to exploit the asymptotic sparsity, we used WHT matrix rows as expansion coefficients $\{\phi_i[n]\}_{i=1}^M$ of demodulating functions $\{z_i(t)\}_{i=1}^M$, which cyclically repeat with period $\tau = NT$. The rows were picked in the multilevel-subsampling fashion [49], [50]. We selected $\log_2(N)$ sampling levels and the number of rows in the measurement matrix assigned to the j -th level is 2^{j-1} , for $j = 1, \dots, \log_2(N)$. The amount of measurement vectors picked in each sampling level M_j was uniformly assigned, i.e. $M_j = M/\log_2(N)$. Let us denote the set of indices corresponding to the j -th sampling level as $\mathcal{U}_j = \{U_{j-1}+1, \dots, U_j\}$, where $0 < U_1 < \dots < U_{\log_2(N)}$, and $N = \sum_{j=1}^{\log_2(N)} \mathcal{U}_j$. Indices corresponding to the picked rows were $\Omega_j \subseteq \{U_{j-1}+1, \dots, U_j\}$, $|\Omega_j| = M_j$, and had been chosen uniformly at random. In case when $M_j > U_j - U_{j-1}$, the residual was transferred to the next sampling level.

In our experimental settings, we selected the rate of innovation of demodulating signals to be 8 times lower than the sampling rate of the original audio signal, and consequently the rate of innovation of a reconstructed signal was $\rho = 1/T = 24$ kHz. The amount of coefficients corresponding to a single interval was set to $N = 1024$, leading to a system with a sampling rate $M/(NT)$, where the number of channels was $M < N$. Furthermore, in order to simulate the analog integration, we interpolated the high-resolution audio signal by the zero-order hold model. Such a model is sufficient since the sampling rate of 192 kHz is a lot higher than the highest frequency of interest in audio signals and since the integration interval duration $\tau = NT$ is much longer than T . Moreover, the small discrepancies can be modeled as the measurement noise.

The audio signal was reconstructed from a reduced set of measurements by using the two proposed methods, namely the method with discrete-time correction filtering that follows the CS recovery (see Section V) and the generalized method with an embedded correction filter (see Section VI). We simulated every setting 20 times for various indices Ω_j and calculated the mean of reconstruction results. The quality of reconstructions in terms of SNR are given in Fig. 8. In Fig. 8a and Fig. 8b, the graphs show that for both the reconstruction methods, representations of the signal in B-spline subspaces of degree $p > 0$ achieve much better reconstruction results than the representation with the B-spline of degree $p = 0$,

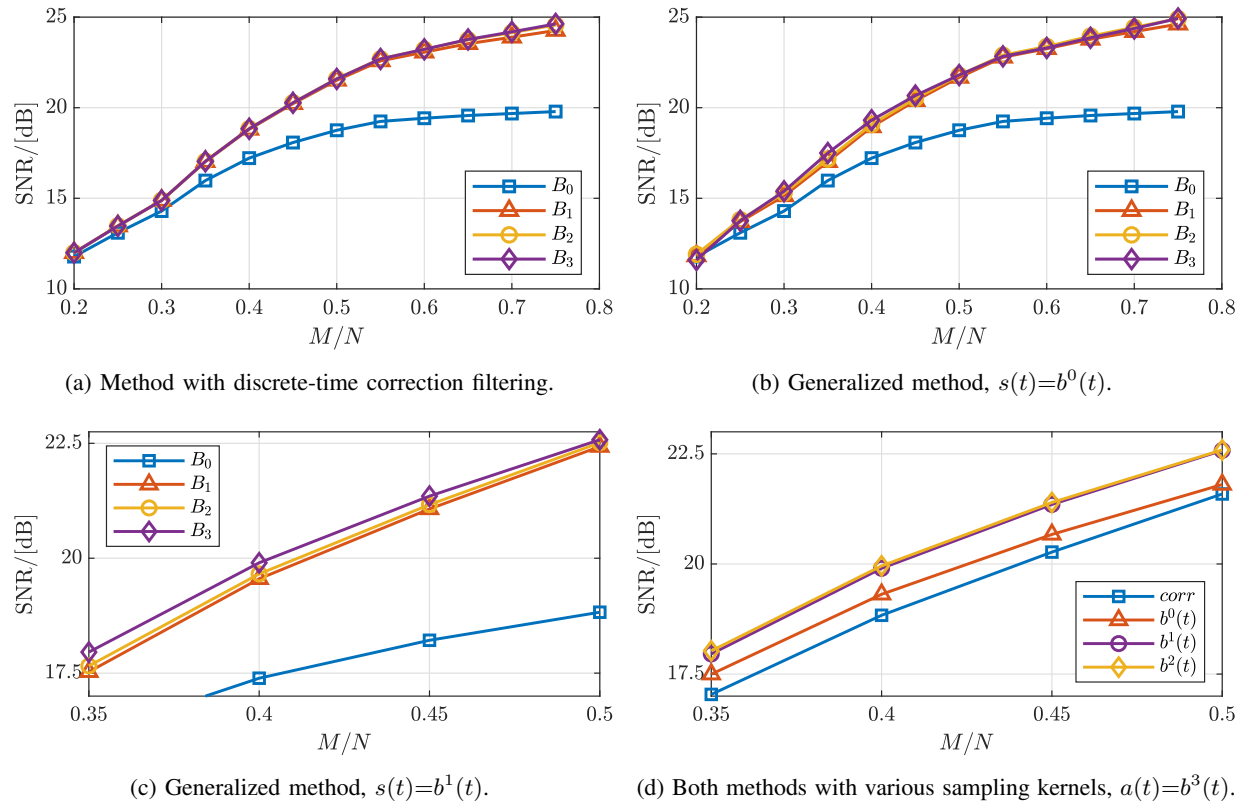


Fig. 8. **Reconstruction results of a real-world signal.** (a), (b) and (c) Reconstruction quality for various measurement settings and reconstruction methods in which the signal was assumed to lie in B-spline subspaces of degree $0, \dots, 3$. (d) Comparison of reconstruction results of the two methods, namely the one with discrete time correction filtering (*corr*) and the generalized method. We used B-spline sampling kernels $s(t)$ of degrees 0, 1 and 2, and the signal generator $a(t)$ was assumed to lie in the B-spline subspace of degree 3.

which can be seen as the traditional CS method. That is, the parametric models obtained directly by the proposed reconstruction methods represent signals much better than the samples obtained by the traditional discrete method. Fig. 8c shows that as we increase the degree of a B-spline generator $a(t)$, we can accordingly expect higher SNR of a reconstruction. This is due to the support of the B-spline basis functions, which expands as the degree increases. Thus, the coefficients are recovered from additional information from neighboring intervals and the model asymptotically approaches the *sinc* reconstruction formula that fits audio signals.

The results in Fig. 8d show that the generalized method with an embedded correction filter outperforms the method with discrete-time filtering. The method with discrete-time filtering recovers exactly N SI samples which are later additionally filtered with an amplifying correction filter from Table I.

Contrarily, the generalized method directly recovers $L \geq N$ expansion coefficients, which is caused by the overlapping basis functions from the neighboring intervals. Thus, the latter method improves a recovery and mitigates the blocking artifacts. While the blocking artifacts are usually avoided by complex postprocessing methods, the proposed generalized method possesses the ability to reject them within the CS recovery procedure. Even though the difference between reconstruction qualities of the two methods are apparent from the SNR values, the ability to mitigate the blocking artifacts additionally enhances the reconstruction quality of the generalized method.

Finally, the generalized method offers measurements with arbitrary sampling kernels $s(t)$ and Fig. 8d shows that the sampling kernels of degree 1 and 2 outperform the standard RD-based measurements with a sampling kernel of degree 0.

VIII. CONCLUSION

We proposed a framework for sampling and reconstruction of signals in shift-invariant spaces whose expansion coefficients are assumed to be sparse in a certain transform domain. Two reconstruction methods based on a combination of compressive sensing and the shift-invariant reconstruction procedure were introduced. The methods allow for reconstruction of sparse signals from a much lower sampling rate in contrast to the traditional shift-invariant setting. We have shown that such an inherently continuous-domain inverse problem can be discretized into a finite-dimensional problem of compressive sensing type in an exact way. We implemented the proposed methods for sampling and reconstruction of signals in B-spline spaces. Numerical experiments proved that our methods are robust and a perfect reconstruction of ideally Q -sparse signals in B-spline spaces is achievable. Good reconstruction results are promising for acquisition of real-world signals, images and multidimensional signals that goes beyond the traditional limits.

APPENDIX A

Entries $\tilde{R}_{n,m}$ of the matrix $\tilde{\mathbf{R}}$ are determined by calculating the integral

$$\tilde{R}_{n,m} = \int_{k\tau}^{(k+1)\tau} a(t - mT)s(t - nT)dt. \quad (30)$$

For simplicity, we set the period of the functions to $T = 1$ and the index k to 0. We choose $N = 32$ and the generators $s(t)$ and $a(t)$ are both B-splines of degree 1. Shift-invariant subspaces \mathcal{A} and \mathcal{S} are identical and are spanned by $\{a(t - m)\}$ and $\{s(t - n)\}$, respectively. The SI subspace \mathcal{A} is illustrated in Fig. 9. The function $a(t + 1)$ corresponds to the left integration interval ($k = -1$), but it overlaps the boundary and impacts the integration in the observed interval ($k = 0$). Analogously, the function

$a(t - 32)$ overlaps the right boundary. The sampling functions $\{s(t - n)\}$ act the same way. Thus, the matrix $\tilde{\mathbf{R}}$ is an $H \times L = (N + 2) \times (N + 2)$ dimension matrix with entries:

$$\tilde{\mathbf{R}} = \begin{bmatrix} \frac{1}{24} & \frac{1}{12} & 0 & 0 & 0 & \cdots & 0 \\ \frac{1}{12} & \frac{15}{24} & \frac{1}{6} & 0 & 0 & \cdots & 0 \\ 0 & \frac{1}{6} & \frac{2}{3} & \frac{1}{6} & 0 & \cdots & 0 \\ \vdots & \cdots & \ddots & \ddots & \ddots & \cdots & 0 \\ 0 & \cdots & 0 & \frac{1}{6} & \frac{2}{3} & \frac{1}{6} & 0 \\ 0 & \cdots & 0 & 0 & \frac{1}{6} & \frac{15}{24} & \frac{1}{12} \\ 0 & \cdots & 0 & 0 & 0 & \frac{1}{12} & \frac{1}{24} \end{bmatrix}. \quad (31)$$

Notice that the entries on the diagonal repeat when we move away from the corners and they are equal to the nonzero values of the cross-correlation sequence $r_{sa}[n] = [\dots, 0, 1/6, \underline{2/3}, 1/6, 0, \dots]$.

APPENDIX B

In our example, we consider the concatenation of B-spline expansion coefficients of order 1. For simplicity, we set the period of the functions to $T = 1$ and index k to 0. Two basis functions, namely $a(t + 1)$ and $a(t - N)$, overlap the integration interval, one at the left and another at the right boundary of the integration interval. Thus, the recovered vector of expansion coefficients is $\hat{\mathbf{d}}_0 \in \mathbb{R}^L$, where $L = N + 2$. Previously, we recovered the vector of expansion coefficients $\hat{\mathbf{d}}_{-1} \in \mathbb{R}^L$ for the interval when $k = -1$. The last two entries in $\hat{\mathbf{d}}_{-1}$ and the first two entries in $\hat{\mathbf{d}}_0$ characterizes the same two expansion coefficients, namely $d[-1]$ and $d[0]$. In order to determine $d[-1]$ and $d[0]$, we apply the weighted average

$$d[-1] = w_2 \hat{d}_{-1, L-1} + w_1 \hat{d}_{0, 1} \quad (32)$$

$$d[0] = w_1 \hat{d}_{-1, L} + w_2 \hat{d}_{0, 2}, \quad (33)$$

where w_i are the weights. The weights are efficiently calculated from the entries of the matrix $\tilde{\mathbf{R}}$. The weights are equal to the sum of the entries in the first $L - N$ columns of $\tilde{\mathbf{R}}$. In the case when the generator

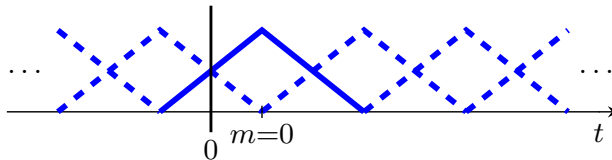


Fig. 9. Shift-invariant subspace \mathcal{A} spanned by $\{a(t - m)\}$. The left boundary of the integration interval is the black line at $t = 0$. The generator $a(t)$ is illustrated by solid lines and its integer shifts by dashed lines.

$a(t)$ is the B-spline of degree 1, $L - N = 2$ and the weights are $w_1 = 1/8$ and $w_2 = 7/8$. Notice that the weights correspond to the amount of area under the basis functions in the observed integration interval and using the matrix $\tilde{\mathbf{R}}$ is just an efficient and elegant way of calculating the areas.

REFERENCES

- [1] H. Nyquist, "Certain topics in telegraph transmission theory," *Transactions of the American Institute of Electrical Engineers*, vol. 47, no. 2, pp. 617–644, Apr. 1928.
- [2] C. E. Shannon, "Communication in the presence of noise," *Proceedings of the IRE*, vol. 37, no. 1, pp. 10–21, Jan. 1949.
- [3] I. Daubechies, "The wavelet transform, time-frequency localization and signal analysis," *IEEE Transactions on Information Theory*, vol. 36, no. 5, pp. 961–1005, 1990.
- [4] M. Unser, "Splines: A perfect fit for signal and image processing," *IEEE Signal Processing Magazine*, vol. 16, no. 6, pp. 22–38, 1999.
- [5] —, "Sampling-50 years after Shannon," *Proceedings of the IEEE*, vol. 88, no. 4, pp. 569–587, Apr. 2000.
- [6] P. Vaidyanathan, "Generalizations of the sampling theorem: Seven decades after Nyquist," *IEEE Transactions on Circuits and Systems I: Fundamental Theory and Applications*, vol. 48, no. 9, pp. 1094–1109, 2001.
- [7] Y. C. Eldar and T. Michaeli, "Beyond bandlimited sampling," *IEEE Signal Processing Magazine*, vol. 26, no. 3, pp. 48–68, May 2009.
- [8] E. Candes, J. Romberg, and T. Tao, "Robust uncertainty principles: Exact signal reconstruction from highly incomplete frequency information," *IEEE Transactions on Information Theory*, vol. 52, no. 2, pp. 489–509, Feb. 2006.
- [9] D. Donoho, "Compressed sensing," *IEEE Transactions on Information Theory*, vol. 52, no. 4, pp. 1289–1306, Apr. 2006.
- [10] E. Candes and M. Wakin, "An introduction to compressive sampling," *IEEE Signal Processing Magazine*, vol. 25, no. 2, pp. 21–30, Mar. 2008.
- [11] S. Foucart and H. Rauhut, *A Mathematical Introduction to Compressive Sensing*. Springer New York, 2013.
- [12] B. Adcock, A. C. Hansen, C. Poon, and B. Roman, "Breaking the coherence barrier: A new theory for compressed sensing," *Forum of Mathematics, Sigma*, vol. 5, 2017.
- [13] E. J. Candès, "The restricted isometry property and its implications for compressed sensing," *Comptes Rendus Mathématique*, vol. 346, no. 9-10, pp. 589–592, May 2008.
- [14] L. Stankovic, D. P. Mandic, M. Dakovic, and I. Kisil, "Demystifying the coherence index in compressive sensing [lecture notes]," *IEEE Signal Processing Magazine*, vol. 37, no. 1, pp. 152–162, Jan. 2020.
- [15] E. Crespo Marques, N. Maciel, L. Naviner, H. Cai, and J. Yang, "A review of sparse recovery algorithms," *IEEE Access*, vol. 7, pp. 1300–1322, 2019.
- [16] Y. C. Eldar and M. Mishali, "Robust recovery of signals from a structured union of subspaces," *IEEE Transactions on Information Theory*, vol. 55, no. 11, pp. 5302–5316, Nov. 2009.
- [17] B. Adcock and A. C. Hansen, "Generalized sampling and infinite-dimensional compressed sensing," *Foundations of Computational Mathematics*, vol. 16, no. 5, pp. 1263–1323, Aug. 2016.
- [18] B. Adcock, "Infinite-dimensional compressed sensing and function interpolation," *Foundations of Computational Mathematics*, vol. 18, no. 3, pp. 661–701, Apr. 2018.
- [19] T. Vlašić, J. Ivanković, A. Tafro, and D. Seršić, "Spline-like Chebyshev polynomial representation for compressed sensing," in *2019 11th International Symposium on Image and Signal Processing and Analysis (ISPA)*, Sep. 2019.
- [20] T. Vlašić, I. Ralašić, A. Tafro, and D. Seršić, "Spline-like Chebyshev polynomial model for compressive imaging," *Journal of Visual Communication and Image Representation*, vol. 66, p. 102731, Jan. 2020.

- [21] M. Mishali and Y. Eldar, “Blind multiband signal reconstruction: Compressed sensing for analog signals,” *IEEE Transactions on Signal Processing*, vol. 57, no. 3, pp. 993–1009, Mar. 2009.
- [22] R. T. Yazicigil, T. Haque, M. R. Whalen, J. Yuan, J. Wright, and P. R. Kinget, “Wideband rapid interferer detector exploiting compressed sampling with a quadrature analog-to-information converter,” *IEEE Journal of Solid-State Circuits*, vol. 50, no. 12, pp. 3047–3064, Dec. 2015.
- [23] F. Pareschi, P. Albertini, G. Frattini, M. Mangia, R. Rovatti, and G. Setti, “Hardware-algorithms co-design and implementation of an analog-to-information converter for biosignals based on compressed sensing,” *IEEE Transactions on Biomedical Circuits and Systems*, vol. 10, no. 1, pp. 149–162, Feb. 2016.
- [24] M. Pelissier and C. Studer, “Non-uniform wavelet sampling for RF analog-to-information conversion,” *IEEE Transactions on Circuits and Systems I: Regular Papers*, vol. 65, no. 2, pp. 471–484, Feb. 2018.
- [25] K. Sever, T. Vlačić, and D. Seršić, “A realization of adaptive compressive sensing system,” in *2020 43rd International Convention on Information and Communication Technology, Electronics and Microelectronics (MIPRO)*, Oct. 2020. [Online]. Available: http://docs.mipro-proceedings.com/proceedings/mipro_2020_proceedings.pdf
- [26] E. J. Candès and C. Fernandez-Granda, “Towards a mathematical theory of super-resolution,” *Communications on Pure and Applied Mathematics*, vol. 67, no. 6, pp. 906–956, Apr. 2013.
- [27] C. Aubel, D. Stotz, and H. Bölcskei, “A theory of super-resolution from short-time fourier transform measurements,” *Journal of Fourier Analysis and Applications*, vol. 24, no. 1, pp. 45–107, Apr. 2017.
- [28] Q. Denoyelle, V. Duval, and G. Peyré, “Support recovery for sparse super-resolution of positive measures,” *Journal of Fourier Analysis and Applications*, vol. 23, no. 5, pp. 1153–1194, Oct. 2017.
- [29] M. Vetterli, P. Marziliano, and T. Blu, “Sampling signals with finite rate of innovation,” *IEEE Transactions on Signal Processing*, vol. 50, no. 6, pp. 1417–1428, Jun. 2002.
- [30] P. L. Dragotti, M. Vetterli, and T. Blu, “Sampling moments and reconstructing signals of finite rate of innovation: Shannon meets Strang–Fix,” *IEEE Transactions on Signal Processing*, vol. 55, no. 5, pp. 1741–1757, May 2007.
- [31] T. Blu, P.-L. Dragotti, M. Vetterli, P. Marziliano, and L. Coulot, “Sparse sampling of signal innovations,” *IEEE Signal Processing Magazine*, vol. 25, no. 2, pp. 31–40, Mar. 2008.
- [32] J. A. Tropp, J. N. Laska, M. F. Duarte, J. K. Romberg, and R. G. Baraniuk, “Beyond Nyquist: Efficient sampling of sparse bandlimited signals,” *IEEE Transactions on Information Theory*, vol. 56, no. 1, pp. 520–544, Jan. 2010.
- [33] T. Vlačić and D. Seršić, “Sub-Nyquist sampling in shift-invariant spaces,” in *2020 28th European Signal Processing Conference (EUSIPCO)*, Aug. 2020. [Online]. Available: <https://www.eurasip.org/Proceedings/Eusipco/Eusipco2020/pdfs/0002284.pdf>
- [34] J. N. Laska, S. Kirolos, M. F. Duarte, T. S. Ragheb, R. G. Baraniuk, and Y. Massoud, “Theory and implementation of an analog-to-information converter using random demodulation,” in *2007 IEEE International Symposium on Circuits and Systems*, May 2007.
- [35] M. Mishali and Y. Eldar, “From theory to practice: Sub-Nyquist sampling of sparse wideband analog signals,” *IEEE Journal of Selected Topics in Signal Processing*, vol. 4, no. 2, pp. 375–391, Apr. 2010.
- [36] M. Mishali, Y. C. Eldar, and A. J. Elron, “Xampling: Signal acquisition and processing in union of subspaces,” *IEEE Transactions on Signal Processing*, vol. 59, no. 10, pp. 4719–4734, Oct. 2011.
- [37] Y. C. Eldar, “Compressed sensing of analog signals in shift-invariant spaces,” *IEEE Transactions on Signal Processing*, vol. 57, no. 8, pp. 2986–2997, Aug. 2009.
- [38] M. Mishali and Y. Eldar, “Reduce and boost: Recovering arbitrary sets of jointly sparse vectors,” *IEEE Transactions on Signal Processing*, vol. 56, no. 10, pp. 4692–4702, Oct. 2008.

- [39] M. Unser, J. Fageot, and J. P. Ward, “Splines are universal solutions of linear inverse problems with generalized TV regularization,” *SIAM Review*, vol. 59, no. 4, pp. 769–793, Jan. 2017.
- [40] H. Gupta, J. Fageot, and M. Unser, “Continuous-domain solutions of linear inverse problems with Tikhonov versus generalized TV regularization,” *IEEE Transactions on Signal Processing*, vol. 66, no. 17, pp. 4670–4684, Sep. 2018.
- [41] T. Debarre, J. Fageot, H. Gupta, and M. Unser, “B-spline-based exact discretization of continuous-domain inverse problems with generalized TV regularization,” *IEEE Transactions on Information Theory*, vol. 65, no. 7, pp. 4457–4470, Jul. 2019.
- [42] T. Debarre, S. Aziznejad, and M. Unser, “Hybrid-spline dictionaries for continuous-domain inverse problems,” *IEEE Transactions on Signal Processing*, vol. 67, no. 22, pp. 5824–5836, Nov. 2019.
- [43] P. Bohra and M. Unser, “Continuous-domain signal reconstruction using L_p -norm regularization,” *IEEE Transactions on Signal Processing*, vol. 68, pp. 4543–4554, 2020.
- [44] M. Unser, A. Aldroubi, and M. Eden, “B-spline signal processing. I. Theory,” *IEEE Transactions on Signal Processing*, vol. 41, no. 2, pp. 821–833, 1993.
- [45] —, “B-spline signal processing. II. Efficiency design and applications,” *IEEE Transactions on Signal Processing*, vol. 41, no. 2, pp. 834–848, 1993.
- [46] D. L. Donoho, “For most large underdetermined systems of linear equations the minimal ℓ_1 -norm solution is also the sparsest solution,” *Communications on Pure and Applied Mathematics*, vol. 59, no. 6, pp. 797–829, 2006.
- [47] Y. C. Eldar, *Sampling Theory*. Cambridge University Press, 2015.
- [48] R. Baraniuk, M. Davenport, R. DeVore, and M. Wakin, “A simple proof of the restricted isometry property for random matrices,” *Constructive Approximation*, vol. 28, no. 3, pp. 253–263, Jan. 2008.
- [49] B. Roman, A. Hansen, and B. Adcock, “On asymptotic structure in compressed sensing,” 2014, arXiv:1406.4178.
- [50] F. Krahermer and R. Ward, “Stable and robust sampling strategies for compressive imaging,” *IEEE Transactions on Image Processing*, vol. 23, no. 2, pp. 612–622, Feb. 2014.
- [51] A. Sović Kržić and D. Seršić, “L1 minimization using recursive reduction of dimensionality,” *Signal Processing*, vol. 151, pp. 119–129, Oct. 2018.
- [52] S. Brugiapaglia and B. Adcock, “Robustness to unknown error in sparse regularization,” *IEEE Transactions on Information Theory*, vol. 64, no. 10, pp. 6638–6661, Oct. 2018.
- [53] J. Mairal. (2020, Sep.) SPAMS—Sparse modeling software. Accessed: Oct. 14, 2020. [Online]. Available: <http://spams-devel.gforge.inria.fr/>
- [54] T. Wik and Barokkanerne, “Vivaldi Cantata RV 679: Che giova il sospirar, povero core,” *Bellezza Crudel - VIVALDI*, 2008, [Sound recording]. [Online]. Available: <http://www.2l.no/hires/>